Characterization of the elastocaloric effects in 3D printable silicone

Author: Marc Torres Padilla, mtorrepa28@alumnes.ub.edu
Facultat de Física, Universitat de Barcelona, Diagonal 645, 08028 Barcelona, Spain.

Advisor: Dr. Eduard Vives Santa-Eulalia, eduardvives@ub.edu

Abstract: The elastocaloric effect has been studied in a 3D printable silicone sample submitted to an adiabatic (fast) variation of uniaxial stress. During this process, the sample temperature has been measured by using an infrared camera allowing to obtain thermal maps of the sample surface. With the help of a custom-designed program, the average temperature over a rectangular area has been determined. The estimated adiabatic temperature change is $\Delta T_{\text{ad}} = 0.99°\text{C}$ when the sample is elongated 388% and $\Delta T_{\text{ad}} = -0.75°\text{C}$ when the sample is unstretched back to its original length.

Keywords: Solid state refrigeration, 3D printable silicone, Stress-strain measurements, Elastocaloric effect, Adiabatic temperature change, Mullins effect

SDGs: Clean and sustainable energy, Industry, Innovation and infraestructure, Sustainable cities and communities, Climate action.

I. INTRODUCTION

Refrigeration is a key achievement of the 20th century, vital for modern life. It preserves food and pharmaceuticals, cools data centres and batteries, and regulates temperatures in transportation and buildings. Development of sustainable energy technologies and material recycling plays a crucial role in minimizing the environmental footprint[1]. The advancements are driven by the necessity to regulate the Earth's surface temperature without exacerbating greenhouse gas emissions. Most present cooling technology uses as refrigerant materials, gases with a huge global warming potential (GWP). For instance, the most used hydrofluorocarbon gases (HFCs) show values between GWP=200 and GWP=600. This means that their global warming potential is between 600 and 200 that of CO_2 [2], which is used as a reference corresponding to GWP=1.

Among promising materials for new refrigeration technologies, the so-called caloric materials stand out due to their ability to exchange heat with their surroundings, making them highly suitable for applications [4].

The characterization of the observed caloric effects can be done by determining the isothermal variation in entropy ($\Delta S_{\text{isotherm}}$) or the adiabatic change in temperature (ΔT_{ad}) that occurs when an external generalized force (electric field, magnetic field, and mechanical force) is applied to or removed from a specific material. In general, these effects in solid materials are relatively small, but when the application of the generalized force induces a phase transition, the heat exchanges become much more important.

To date, the most extensively studied caloric effect is the magnetocaloric effect, which is primarily employed in magnetic refrigeration. This phenomenon involves inducing a first- or second-order phase transition in a solid material through the application of a magnetic field. However, one of the main drawbacks of this approach is the requirement for strong magnetic fields, which necessitate either high electrical currents or the use of permanent magnets made from costly rare-earth elements. [3]

Among the different caloric effects, the elastocaloric effect associated with the application of a uniaxial stress is, apriori, more practical for domestic applications since mechanical forces are much easier to apply than magnetic or electric fields. Moreover, some materials with elastocaloric effects are rather soft. These include polymers, an more specifically, elastomers. For these highly deformable materials, the elastocaloric effect occurs as uniaxial stretching aligns polymer chains and induces a collective phenomenon (similar to a first-order phase transition), known as strain induced crystallization (SIC) [5]. This strongly reduces the conformational entropy of the system which is the underlying reason for the observed large elastocaloric effect in some elastomers.

Materials near first-order phase transitions often display metaestable states, especially in the presence of intrinsic disorder such as impurities, vacancies, dislocations, grain boundaries, sample surfaces, and edges [11]. This may represent a drawback for many caloric applications based on cycling devices since the thermodynamic trajectories become hysteretic with unavoidable losses. The understanding, the control and the possibility of tuning hysteresis is fundamental to improving caloric performances. Besides, metaestables dynamics in the presence of disorder often become intermittent, resulting in avalanche-like behavior, which should be considered especially for small devices working at high frequencies.

At present, the most promising elastomer for sustainable cooling applications is natural rubber. When crossing the SIC transition in adiabatic conditions it shows temperature changes of the order of $\Delta T_{ad} = 10°\text{C}$ [6]. Unlike other caloric materials, natural rubber is flexible, affordable, and biodegradable, making it a viable solution to some of the present engineering and sustainability challenges associated with artificial heating and cooling

systems. Nevertheless, a known problem with NR is its elaboration. Even though it is easy to synthesize and, later, recycle, it is difficult to cut and shape in complex geometries, since its elaboration requires a thermomechanical process (high temperature and high pressure) called vulcanization that does not permit complex molding [7].

q30' 7*/ 'yAnother elastomer with similar mechanical properties is silicone. In this case, it has the advantage that it can be 3D printed in any desirable shape and size and can also be mass produced.

The aim of the present work is to characterize experimentally the adiabatic temperature change ΔT_{ad} corresponding to a 3D printable silicone sample. This will be measured using infrared (IR) techniques in order to map the sample surface temperature, while applying uniaxial stress cycles at different speeds.

In section II we present the details of the experiments that have been performed in the Materials and Phase transitions lab of the Condensed Matter Physics Department. In section III we detail the main results, and finally in section IV, we summarize and conclude.

II. EXPERIMENT

A. Sample

The studied material is a medical-grade liquid silicone rubber (LSR) from Elkem Silicones, AMSil Silbione™, Shore 70A. that can be easilly used in a injection 3D printer. A silicone film was prepared by mixing the two components in a 1:1 ratio and casting it in a sheet shape with 1 mm thickness. This process was done by Dr.E.Xuriguera and Dr.P.Parcelona from the DIOPMA lab in the Chemistry Faculty of the University of Barcelona (U.B.). Rectangular samples measuring 50 × 10 mm were cut from the sheet

B. Thermomechanical tests

A schematic representation of the experimental setup is shown in FIG. 1.

All tests were performed on a Zwick/Roell Z005 universal testing machine fitted with a 5 kN load cell offering 0.5 N resolution [8], available in the Functional Materials and Phase Transitions lab in the Physics Faculty of U.B.

The sample was securely clamped by steel grips to ensure stable alignment and consistent loading throughout each cycle. Small silicone sheets were placed between the sample and the steel grips to prevent the damage of the sample when grips are tighten. The vertical displacement of the upper grip is recorded with a resolution of 0.001 mm. This movement is controlled through the TestXpert software with a selected constant speed.

When the sample is in the initial relaxed state, the vertical separation between the grips is $L_0 = 15.642$ mm. Standard experiments consist in submitting the sample to mechanical cycles with four sections. In the first section the sample is stretched with speed v up to L =60.642 mm . This corresponds to a stretching factor $\lambda \equiv L/L_0 = 3.88$. In the second section the length is kept constant for a pause of 120 s. In the third section the sample is unstretched with speed v to the initial length L_0. And in the final section the length is kept constant for another 120 s. We have performed slow experiments at $v = 10$ mm/min and fast experiments at the maximum allowed speed of $v = 3000$ mm/min.

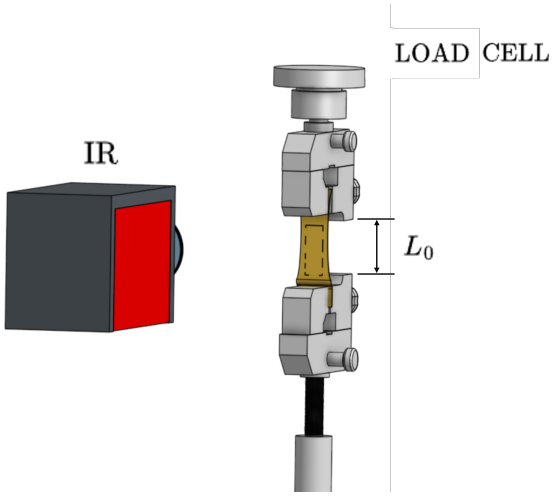

FIG. 1: Diagram of the experimental setup showing the position of the sample in brown color, the grips, the load cell and the IR camera that is placed in front of the sample.

A Thermographic infrared camera (InfraTec 8800) [9] was mounted and focused in front of the specimen to capture two-dimensional thermal maps of its surface. Images are recorded at 100 frames per second ($\Delta t = 0.01$ s) with a spatial resolution of 18.3 pixels/mm and a nominal thermal sensitivity of 35 mK. The camera is controlled through the IRBIS 3.1 Software [10].

To reduce the influence of ambient infrared interferences, the entire setup was enclosed with expanded polystyrene panels acting as an homogeneous thermal barrier, thereby stabilizing the environmental temperature around the specimen during measurements.

Three examples of thermal maps are shown in Fig. 2. They correspond to frames obtained during the shrinkage of the sample in a fast experiment, so that the sample cools to temperatures below room temperature.

Average surface temperature estimates were obtained by averaging pixel values within a rectangular window of interest. This window adjusts its size and position to remain centered on the specimen and scale proportionally as the sample deforms over time. To perform this numerical analysis we have prepared a FORTRAN code that reads the thermal maps, generates the rectangular window and calculates the average temperature and its standard deviation on the selected pixels. The example

in Fig.2 illustrated the rectangles used in the three different recorded thermal maps.

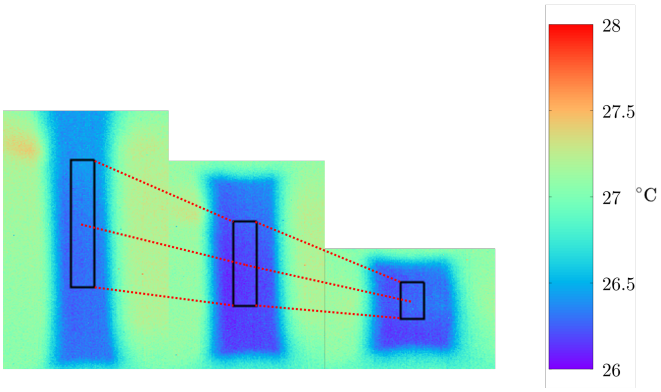

FIG. 2: Three snapshots of the temperature map of the specimen surface during the unstretching section of a fast experiment. The black rectangle indicates the rectangular window where the average temperature is measured. The color temperature scale is indicated on the right hand side.

III. RESULTS

A. Mechanical response

A first special test consisting in several cycles at v =10mm/min has been performed in order to characterize the repeatability of the mechanical behavior of the sample. The sample is stretched to a certain variable deformation. Then, it is returned to the original size, using the same speed as before. For this special test, we have selected 3 different stretching factors. For each deformation, a total of 3 identical consecutive cycles have been performed, all of them at the same speed as mentioned before. The studied stretching factors are $\lambda = L/L_0 =$ 2.5, 3.2 and 3.8, as shown in FIG. 3. The first time that the sample is stretched to a new length, never visited before, the force is much larger than in all the subsequent loops to that same length. This memory effect of the previous maximum deformation is called the Mullins effect[12].

This effect is not completely understood. Several mechanisms for the different behaviour of the first excursion to new lengths have been proposed (bond rupture, polymer slipping, filler rupture, disentanglement, ...) but none of them has been supported unanimously[12]. The experimental data presented in the next subsection, will correspond to elongations that have already been visited before, in order to avoid the Mullins effect.

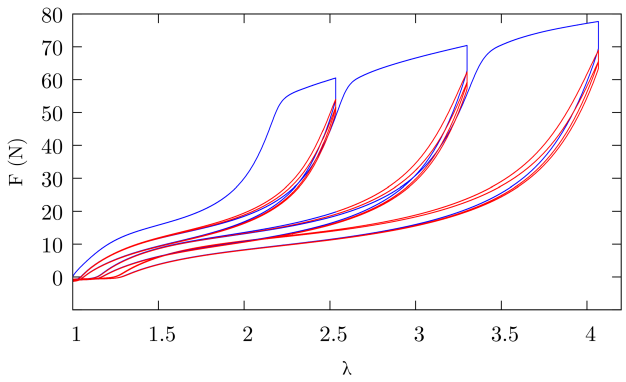

FIG. 3: Force vs. stretching factor behaviour obtained cycling 3 times up to 3 different deformations (λ =2.5, 3.2, 3.8). For each new deformation we indicate, in blue, the first cycle and, in red, the other two.

B. Thermal response

As explained before, for the characterization of the thermal response of the sample, two kinds of stretching - unstretching tests have been performed, at a slow speed of v =10 mm/min, and at a high speed of v =3000 mm/min. In both cycles, the stretching factor is $\lambda = L/L_0 = 3.88$.

1. *Fast cycle*

Results corresponding to the fast cyle are collected in Fig.4. Given the low thermal conductivity of silicone, during the fast stretching or unstretching section, there is no time to exchange heat with the environment. This fast experiment, therefore, corresponds to approximately adiabatic conditions, thus maximizing the temperature change of the sample.

Note that the pause of 120 s separates the stretching and unstretching sections in order recover thermal equilibrium with the environment as can be seen in panel 4(c). After the fast stretching we obtain the maximum sample overheating, and after the unstretching the maximum sample undercooling, as indicated with double arrows.

The measured temperature changes are ΔT_{ad} =0.989°C after stretching, and ΔT_{ad} = -0.747°C after unstretching. The stochastic errors, corresponding to the fact that we are measuring the temperature as an average over a rectangular region on the sample surface, are smaller than 0.001 ° C, and smaller than the width of the line in FIG.4 (c), so they are not shown in the plot. In the next subsection, nevertheless, we will obtain a better estimation of the error bar.

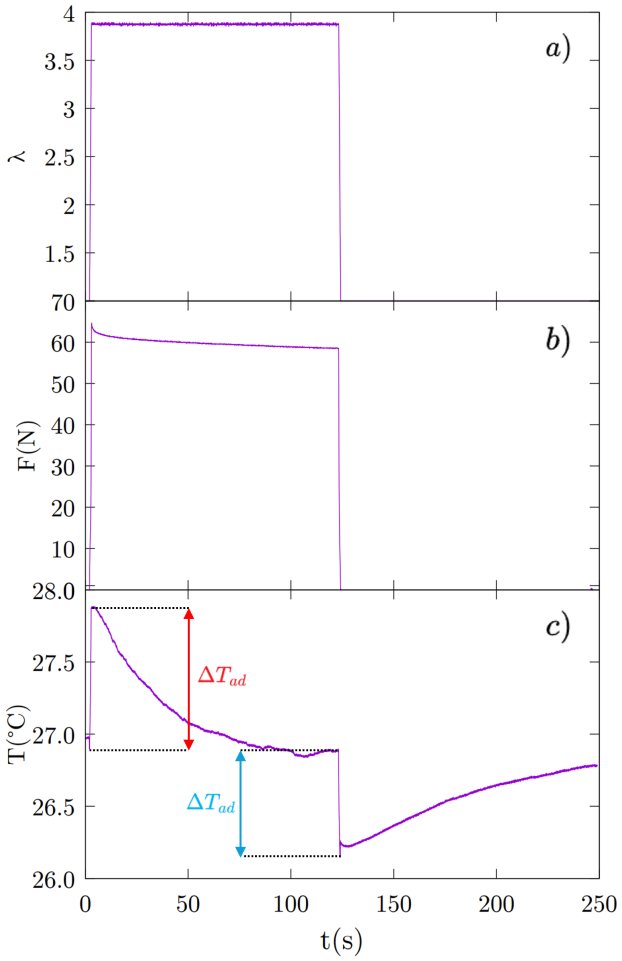

FIG. 4: (a) Time evolution of the streching factor (controlled by the materials testing machine) during the fast experiment; (b) time evolution of the measured applied force; and (c) time evolution of the average surface temperature determined from the IR measurements. In panel (c), we also indicate with arrows the adiabatic temperature changes after stretching (in red), and after unstretching (in blue).

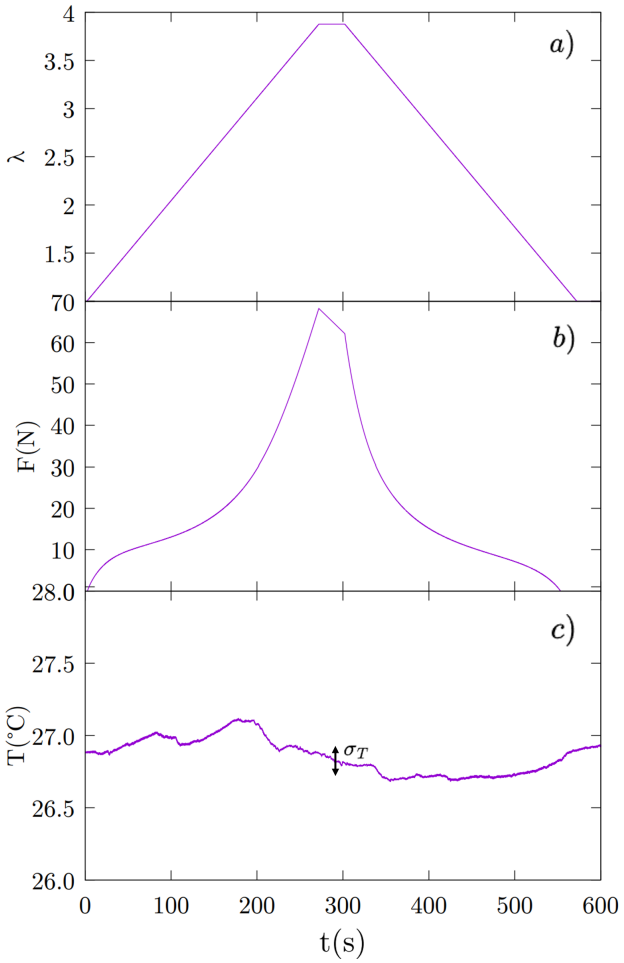

FIG. 5: (a) Time evolution of the stretching factor (controlled by the materials testing machine) during the slow experiment, (b) time evolution of the measured applied force and (c) time evolution of the average surface temperature determined from the IR measurements. In panel (c), we also indicate with a double arrow the standard deviation.

2. *Slow cycle*

The slow experiment, at $v = 10$mm/min, allows us to study the experimental temperature fluctuations caused by many different origins: for instance, the emissivity of the sample surface can be altered when the sample deforms; there can also be angular variations during the experiment that might affect the IR radiation received by the camera, random fluctuations of the evironment temperature, etc. Results are compiled in Fig.5 This cycle is supposed to be slow enough so the sample can be considered in thermal equilibrium with the environment. Thus one can obtain an upper bound of the experimental errors. By computing the standard deviation of the curve in Fig. 5 (c), we obtain $\sigma_T = 0.12$ °C.

This error bar,therefore, is a much better estimation of the stochastic error bars determined in the previous subsection for the adiabatic temperature changes.

IV. SUMMARY AND CONCLUSIONS

We have studied the elastocaloric effect in a 3D printable silicone sample, which has been analyzed in a stretching-unstretching experiment. We have characterized its mechanical and thermal behavior. In the force vs. stretching factor representation, we have demonstrated the so called Mullins effect that occurs when the sample visits values of the stretching factor that have never been visited before.

Evolution of the surface temperature maps have been obtained by IR imaging on stretching and unstretching experiments avoiding the Mullins effect. An average of the temperature in a rectangular window placed inside

the sample has been used. The results are summarized in Figure 6, in which the surface temperature is indicated by the color scale on the F vs. λ plot. The maximum adiabatic temperature change obtained during the stretching section is $\Delta T_{ad} = 0.99 \pm 0.12$ °C; while the corresponding value during the unstretching section is ΔT_{ad} = -0.75 $\pm$ 0.12 °C. A slow experiment (Fig.6, inset), in which the sample is approximately in thermal equilibrium with the environment, has allowed us to obtain an upper bound of the temperature fluctuations of the sample surface when being deformed. The standard deviation is $\sigma_T = 0.12$ °C which is used as an upper bound of the error bars.

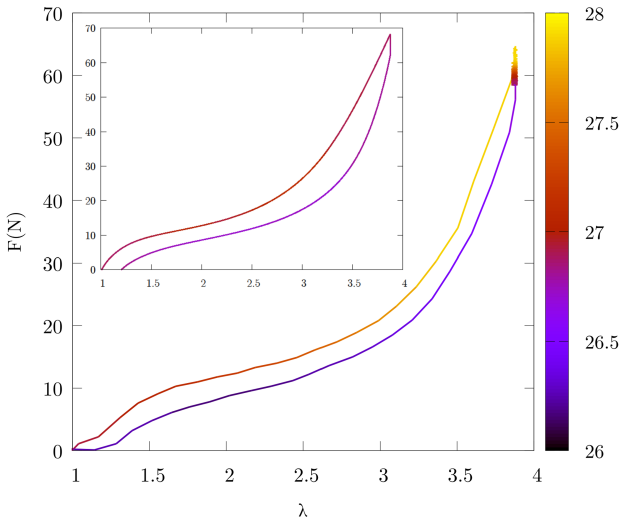

FIG. 6: Behaviour of the force as a function of the stretching factor. The color indicates the corresponding average surface temperature . The main panel corresponds to the fast experiment (adiabatic stretching and unstretching), and the inset to the slow experiment which is perforemd, approximately, in isothermal conditions.

The results reinforce the potential of using silicone as a elastocaloric material in future sustainable cooling systems, without relying on harmful refrigerants. Silicone shows the capacity to induce thermal changes through mechanical stimuli. Moreover, the fact that can be 3D printed, opens the possibility to use silicone as a refrigerant material with a complex shape with a large surface to volume ratio that will allow for fast heat exchanges. Thus silicone is a promising candidate for energy-conscious thermal management technologies.

As a natural extension of the present work, it would be noteworthy to study the behavior of the elastocaloric effect in a 3D printed silicone sample with a non-homogeneous surface. Another idea could be to study different mechanical actuation methods beyond the uniaxial actuation studied here: shear, twisting, compression, biaxial, etc.

Acknowledgments

The author would like to thank Antoni Vives for assistance in the preparation of FIG. 1, as well as express gratitude to close family for their patience and support.

[1] B. Grocholski. "Cooling in a warming world". Science **370**: 776-777 (2020) ed crystallization". Nature Energy **6**: 260-267 (2021).

[2] Ø.Hodnebrog, B.Aamaas, J.S.Fuglestvedt, G.Marston, G.Myhre, C. J. Nielsen, M. Sandstad, K. P. Shine, T. J. Wallington. "Updated Global Warming Potentials and Radiative Efficiencies of Halocarbons and Other Weak Atmospheric Absorbers". Reviews of Geophysics **58**: e2019RG000691 (2020).

[3] Mellari, S. Introduction to magnetic refrigeration: magnetocaloric materials. Int. J. Air-Cond. Ref. **31**, 5 (2023)

[4] Moya, X., Kar-Narayan, S. and Mathur, N. "Caloric materials near ferroic phase transitions". Nature Materials **13**: 439–450 (2014).

[5] Zhang, S., Yang, Q., Li, C. et al. "Solid-state cooling by elastocaloric polymer with uniform chain-lengths". Nature Communications **13**: 9 (2022).

[6] N.Candau, E.Vives, A.I.Fernández-Renna, M.L.Maspoch, "Elastocaloric effect in vulcanized natural rubber and natural/wastes rubber blends", Polymer, **236**: 124309 (2021).

[7] R. Whba, M. Sukor Su'ait, F. Whba, S. Sahinbay, S. Altin, A. Ahmad. "Intrinsic challenges and strategic approaches for enhancing the potential of natural rubber and its derivatives: A review". International Journal of Biological Macromolecules. **276**. Part 1 (2024).

[8] *BZ1-MM14450.ZW01 Zwick Technical Documentation: Instruction Manual (Zwick/Roell, Ulm 2009).*

[9] Infrared-Thermographic Camera ImageIR: User Manual (Infratec GmbH, Dresden, April 2018)

[10] IRBIS 3.1: Infrared Thermographic Software, User Manual (Infratec GmbH, Dresden, April 2018)

[11] A. Planes, A.Saxena, Phase Transitions: A Materials Perspective, (Cambridge University Press, Cambridge, UK,2025, 1st. ed.).

[12] J. Diani, B. Fayolle, P.Gilormini. "A review on the Mullins effect". Eur. Polym. J. **45***: 601-612 (2009)*

Caracterització dels efectes elastocalòrics en silicona imprimible en 3D

Author: Marc Torres Padilla, mtorrepa28@alumnes.ub.edu
Facultat de Física, Universitat de Barcelona, Diagonal 645, 08028 Barcelona, Spain.

Advisor: Dr. Eduard Vives Santa-Eulalia, eduardvives@ub.edu

Resum: S'ha estudiat l'efecte elastocalòric en una mostra de silicona imprimible en 3D sotmesa a una variació adiabàtica (ràpida) de tensió uniaxial. Durant aquest procés, la temperatura de la mostra s'ha mesurat mitjançant una càmera d'infrarojos, la qual ha permès obtenir mapes tèrmics de la seva superfície. Amb l'ajuda d'un programa dissenyat a mida, s'ha determinat la temperatura mitjana sobre una àrea rectangular. El canvi de temperatura adiabàtic estimat és de $\Delta T_{\text{ad}} = 0{,}99\,^{\circ}\text{C}$ quan la mostra s'allarga un 388%, i de $\Delta T_{\text{ad}} = -0{,}75\,^{\circ}\text{C}$ quan la mostra torna a la seva longitud original.
Paraules clau: Refrigeració en estat sòlid, silicona imprimible en 3D, mesures de tensió-deformació, efecte elastocalòric, canvi de temperatura adiabàtic, efecte Mullins.

ODSs: Energia neta i sostenible, Indústria, innovació, infraestructures, Ciutats i comunitats sostenibles, Acció climàtica.

Objectius de Desenvolupament Sostenible (ODSs o SDGs)

1. Fi de la es desigualtats		10. Reducció de les desigualtats	
2. Fam zero		11. Ciutats i comunitats sostenibles	
3. Salut i benestar		12. Consum i producció responsables	
4. Educació de qualitat		13. Acció climàtica	X
5. Igualtat de gènere		14. Vida submarina	
6. Aigua neta i sanejament		15. Vida terrestre	
7. Energia neta i sostenible	X	16. Pau, justícia i institucions sòlides	
8. Treball digne i creixement econòmic		17. Aliança pels objectius	
9. Indústria, innovació, infraestructures	X		

El contingut d'aquest TFG, part d'un grau universitari de Física, està indirectament relacionat amb (i) l'ODS 7 ja que la refrigeració en estat sòlid s'ha proposat com a mètode més eficient que la refrigeració convencional basada en expansió de gasos, energies renovables, ; amb (ii) l'ODS 9, perquè pot representar una innovació en molts processos industrials que requereixen refrigeració; i clarament amb l'ODS 13, perque l'objectiu principal és desenvolupar una tècnica de referdament que eviti l'emissó de gasos que contribueixen a l'efecte hivernacle

GRAPHICAL ABSTRACT